Exploring molecular vibrational motions with periodic orbits

Stavros C. Farantos[a]

[a] Institute of Electronic Structure and Laser, Foundation for Research and Technology-Hellas, and Department of Chemistry, University of Crete, Iraklion, Crete, Greece

PLEASE SCROLL DOWN FOR ARTICLE

Exploring molecular vibrational motions with periodic orbits

by STAVROS C. FARANTOS

Institute of Electronic Structure and Laser,
Foundation for Research and Technology-Hellas,
and Department of Chemistry, University of Crete,
Iraklion, Crete 711 10, Greece

The theory of periodic orbits for conservative Hamiltonian systems and the way that it is applied to analyse vibrational spectra of highly excited polyatomic molecules is reviewed. Applications for triatomic, tetratomic molecules and van der Waals clusters are presented. It is shown that the periodic orbit method can trace localized eigenfunctions above potential barriers which are associated with saddle-node bifurcations. Such states connect separate minima on the potential energy surface, and thus, are important for studying isomerization processes.

1. Introduction: The object of research

Classical mechanics is the theory which describes the motions of macroscopic bodies. Nevertheless, in the last decades of this century classical mechanics has seen an unprecedented popularity among chemical physicists, for whom the main concern is the investigation of molecular motions and transformations.

Since the pioneering work of Karplus, Porter, and Sharma in 1965 on the study of $H + H_2$ reaction [1], the classical trajectory method, and in general classical mechanics, have been applied to a variety of problems ranging from molecular collisions [2], interaction of electromagnetic radiation with atoms and molecules [3], and the simulations of clusters [4] and macroscopic states of matter [5]. Even problems in molecular physics which can be solved quantum mechanically are treated by classical mechanics in an effort to achieve a better physical insight.

One main reason for the adoption of classical mechanical approximation in chemical dynamics is our ability to perform calculations for many-body problems, and to obtain results in good agreement with the experiment.

A general argument for justifying applications of classical mechanics to quantum objects such as molecules, was always referred to the validity of semiclassical theory for heavy particles. At the beginning, the semiclassical quantization rule of Einstein–Brillouin–Keller (EBK) [6, 7] was applied to quantize quasi-periodic trajectories. Dynamical systems whose trajectories in phase space are quasi-periodic are called *integrable*, and that implies that there are as many constants of motion as the number of degrees of freedom [8, 9].

However, the enthusiasm for a theoretical justification of using classical mechanics in molecules was quickly dropped, by realizing that molecular systems are generally not integrable, and thus, at high energies most of the trajectories are *chaotic* for which the EBK semiclassical rule is not valid [10].

The advances of nonlinear classical mechanics and the deeper understanding of the *structure of phase space*, i.e. how regular and chaotic trajectories are interwoven in conservative Hamiltonian systems [11], inevitably brought again the problem of the correspondence of classical to quantum mechanics. Particularly the field of studying

the quantum behaviour of a classically chaotic system has brought much discussion about the meaning of *quantum chaos* [12, 13].

The classical mechanical results for the vibrational motions of a polyatomic molecule are the following. At low energies there is a small deviation from the motions of a few uncoupled harmonic oscillators. These motions are described by quasi-periodic trajectories which lie on the surfaces of tori in phase space, and according to the Kolmogorov–Arnold–Moser (KAM) theorem [14], tori survive even when anharmonicity sets in at higher energies. On the other hand, the same theorem predicts that above some excitation energy, where the anharmonic and coupling terms in the potential function become important, tori are destroyed and chaotic trajectories prevail.

Thus, the generic picture of phase space for small polyatomic molecules which has emerged from all these studies is that, the phase space is predominantly regular at low energies, predominantly chaotic at high energies, and with regular and irregular regions coexisting at intermediate energies. This picture is expected for molecules with one well in the potential energy surface. Most molecules have usually isomers, and this means that the potential energy surfaces have more than one minima separated by saddle points. As we shall see this makes the structure of phase space more complicated.

Now, we ask what is the corresponding quantum mechanical picture of the molecule. Mainly numerical calculations have shown that the eigenfunctions and the distributions of the eigenvalues in quantum mechanical calculations reflect the structure of phase space. For energy ranges where the classical motion is regular the eigenfunctions are localized with well ordered nodal patterns, but for energies where the classical motion is chaotic the eigenfunctions are delocalized with irregular nodal patterns. Similarly, the distributions of the differences of adjacent energy levels are different for energy ranges where the classical motions are regular and chaotic [7, 15].

The most exciting outcome of all these studies was the numerical observation that even in regions of phase space where classical mechanics show chaotic behaviour, quantum wavefunctions may remain localized in configuration space to some extent. This localization was associated with periodic orbits after the pioneering work of McDonald and Kaufman [16], and Heller [17, 18] in the stadium model.

This discovery brought to the light an earlier work by Gutzwiller on the semiclassical calculation of the density of states by using an infinite summation over periodic orbits [19, 20]. Since periodic orbits may be unstable as well as stable, the trace formula of Gutzwiller, as his semiclassical formula is now known, is considered as one way for semiclassically quantizing unstable trajectories [21–27].

Periodic orbits were considered by Poincaré as the most important objects to explore the complicated structure of phase space [28]. The localization of the quantum wavefunctions along the periodic orbits at high excitation energies where the trajectories are most chaotic, has made the periodic orbits important for quantum mechanics as well.

A much studied physical system in association with nonlinear mechanics is the hydrogen atom in strong magnetic fields for which excellent results have been obtained [29–31].

Furthermore, the effort for understanding the classical–quantum correspondence in the light of the new discoveries has triggered a lot of research in molecular vibrational spectroscopy. Polyatomic molecules offer real systems for testing the theories of nonlinear mechanics.

A vibrational spectrum is the fingerprint of the nuclear motions in the molecule. At low-lying energies a typical normal mode analysis is the standard approach for the

assignment of the spectra. Usually, a harmonic Hamiltonian plus a few anharmonic terms treated with perturbation theory, are enough to assign quantum numbers to the observed peaks of the spectrum [32].

A successful assignment of the peaks with good quantum numbers is what is expected for a *regular spectrum*, and this is always true for the first low-energy vibrational levels. However, at high energies complex spectra appear, and then, no assignment of the peaks is possible with good quantum numbers. In such cases statistical methods, which use global functional forms are employed to describe the spectra [15]. These non-assignable spectra are called *irregular* or *chaotic*.

Still, it has been found that an irregular spectrum may show regular patterns at low resolution [33, 34].Then, it is possible to label the peaks of the low-resolution spectrum with normal mode quantum numbers. The significance of the regularities at low resolution can be appreciated when we calculate spectra within a time-dependent theory [35]. The spectrum is then the Fourier transform of a time autocorrelation function that traces the evolution of a wavepacket in time. Recurrences of the wavepacket to its initial position explains the spectroscopic peaks. In turn, we can ask what is the correspondence of the dynamics of wavepacket to the classical trajectories. As was stated before, the similarities between classical and quantum dynamics found for molecular systems are astonishing.

Acetylene [36–38] was the first molecule to be tested for quantum chaotic behaviour. Other molecules such as NO_2 [39, 40], SO_2 [41–43], Na_3 [44, 45], HCN [46, 47], O_3 [48–50], H_3^+ [51, 52], CS_2 [53], SiH_2 [54], CH_2OH [55], H_2CO [56] followed. Molecules which show chaotic behaviour in high-resolution spectroscopy, may have regular assignable spectra in low-resolution spectroscopy.

For theoretical spectroscopy the following questions have to be answered:

> *Given the complexity of polyatomic molecules and the difficulties of carrying out quantum mechanical calculations for many degrees of freedom systems, can we deduce the dynamics from a spectrum?*
> *Even more, can we predict the dynamical behaviour of a molecule for given potential energy surface(s)?*

Classical mechanics seem to offer important tools not only for qualitative answers, but also with a predictive power for the motions of the polyatomic molecules at high energies where nonlinear effects are strong and quantum mechanical calculations difficult to perform. There is no doubt that the final answers to the above questions must be quantum mechanical, and good agreement between quantum and classical mechanics poses the need for the development of a quantum theory compatible with the classical theory of chaos.

In this article we review classical mechanical methods for analysing the nuclear motions in polyatomic molecules referring mainly to our work. A recent review article on the same subject is that of Gomez and Pollak [33]. Here, not only do we cover more recent results, but also we emphasize methods of exploring the molecular phase space structure.

The article is organized in the following manner. § 2 describes how a periodic orbit analysis reveals the structure of phase space. In § 3, we describe methods for obtaining spectra in the classical, semiclassical, and quantum mechanical approximations from particular regions of phase space. Methods for locating periodic orbits, examining their stability, and following their evolution with the energy are presented in § 4. In § 5 applications of the periodic orbit approach will be given for triatomic molecules such

as HCN, O_3, and SO_2, van der Waals clusters, ArCO, Ar_3, as well as tetratomic molecules such as C_2H_2. Finally in § 6, we summarize the conclusions.

2. Periodic orbits and phase space structure

We assume that the molecular *potential energy surface* (pes) of a specific electronic state is known. In the classical mechanical approximation we are interested in investigating the phase space structure for a range of energies. The total energy of the system is a common varying parameter in a nonlinear mechanical search.

With the term phase space structure we mean to search for regions of phase space which contain trajectories of similar type. For example, a coarse graining characterization of phase space is the detection of the regions with quasi-periodic and chaotic trajectories. A more detailed study will reveal which resonance dominates in a certain region of phase space [11]. In this section we discuss how families of periodic orbits portray the structure of phase space.

Let q_i, $i = 1, \ldots, N$, be the generalized coordinates of a dynamical system of N degrees of freedom, and p_i, $i = 1, \ldots, N$, the conjugate momenta. If $H(\mathbf{q}, \mathbf{p})$ is the Hamiltonian of the system, the equations of motion are written in Hamilton's form as,

$$\left. \begin{array}{l} dq_i/dt = \dot{q}_i(t) = \partial H/\partial p_i \\ dp_i/dt = \dot{p}_i(t) = -\partial H/\partial q_i, \quad i = 1, \ldots, N. \end{array} \right\} \tag{1}$$

For convenience, we consider coordinates and momenta as the components of the vector $\mathbf{x}$,

$$\mathbf{x} = (q_1, \ldots, q_N, p_1, \ldots, p_N)^{\mathrm{T}}, \tag{2}$$

where T denotes the transpose of the $2N$-D column vector. The equations of motion are then written,

$$\dot{\mathbf{x}}(t) = \mathbf{J}\, \frac{\partial H(\mathbf{x})}{\partial \mathbf{x}} = \mathbf{J}\, \nabla H(\mathbf{x}), \tag{3}$$

where,

$$\mathbf{J} = \begin{pmatrix} \mathbf{0}_N & \mathbf{I}_N \\ -\mathbf{I}_N & \mathbf{0}_N \end{pmatrix}. \tag{4}$$

$\mathbf{0}_N$ and $\mathbf{I}_N$ are the zero and unit $N \times N$ matrices respectively. $\mathbf{J}\,\nabla H(\mathbf{x})$ is a vector field, and $\mathbf{J}$ a symplectic matrix which satisfies the relations,

$$\mathbf{J}^{-1} = -\mathbf{J}, \quad \text{and} \quad \mathbf{J}^2 = -\mathbf{I}_{2N}. \tag{5}$$

Linearization of the equations of motion is a common strategy to study the behaviour of the trajectories around a specific trajectory $\mathbf{x}(t)$. The Grobman–Hartman theorem [57] states that the linearization of the vector field ($\mathbf{J}\,\nabla H(\mathbf{x})$) is topologically equivalent to the vector field. Thus, important conclusions obtained for the linearized system can be extended to the nonlinear system.

If $\mathbf{x}(t)$ is a solution of equation (3) we want to know the behaviour of a nearby trajectory

$$\mathbf{x}'(t) = \mathbf{x}(t) + \boldsymbol{\zeta}(t). \tag{6}$$

From equation (3) we have,

$$\dot{\mathbf{x}}'(t) - \dot{\mathbf{x}}(t) = \mathbf{J}\,\nabla H(\mathbf{x}') - \mathbf{J}\,\nabla H(\mathbf{x}). \tag{7}$$

A Taylor expansion of the right hand side (r.h.s.) of equation (7) up to the first order gives,

$$\dot{\zeta}(t) = \mathbf{J}\partial^2 H[\mathbf{x}(t)]\zeta(t). \tag{8}$$

$\partial^2 H[\mathbf{x}(t)]$ denotes the matrix of second derivatives of the Hamiltonian evaluated at $\mathbf{x}(t)$. If,

$$\mathbf{A}(t) = \mathbf{J}\partial^2 H[\mathbf{x}(t)], \tag{9}$$

then equation (8) is written as,

$$\dot{\zeta}(t) = \mathbf{A}(t)\zeta(t). \tag{10}$$

These are $2N$ linear differential equations with time dependent coefficients, and are called *variational equations* [58].

The general solution of equation (10) can be expressed by

$$\zeta(t) = \mathbf{Z}(t)\zeta(0), \tag{11}$$

where $\zeta(0)$ describes the initial displacement from the trajectory $\mathbf{x}$. The fundamental matrix, $\mathbf{Z}(t)$, satisfies the variational equations as can be easily proved;

$$\dot{\mathbf{Z}}(t) = \mathbf{A}(t)\mathbf{Z}(t). \tag{12}$$

If $\mathbf{x}(t; \mathbf{s})$ is the reference trajectory with initial conditions $\mathbf{s}$, then we can show that the fundamental matrix has columns the vectors,

$$\mathbf{z}_k = \frac{\partial \mathbf{x}(t; \mathbf{s})}{\partial s_k}, \tag{13}$$

i.e. the derivatives of the trajectory $\mathbf{x}(t; \mathbf{s})$ with respect to the initial coordinates s_k, $k = 1, \ldots, 2N$. Indeed, differentiating both sides of equation (3) we take,

$$\left.\begin{aligned}
\frac{\partial \dot{\mathbf{x}}}{\partial s_k} &= \mathbf{J}\frac{\partial}{\partial s_k}\nabla H, \\
\frac{d}{dt}\left(\frac{\partial \mathbf{x}}{\partial s_k}\right) &= \mathbf{J}(\partial^2 H)\frac{\partial \mathbf{x}}{\partial s_k} \\
&= \mathbf{A}(t)\frac{\partial \mathbf{x}}{\partial s_k}.
\end{aligned}\right\} \tag{14}$$

Thus,

$$\dot{\mathbf{z}}_k = \mathbf{A}(t)\mathbf{z}_k. \tag{15}$$

Obviously, at $t = 0$, $\mathbf{Z}$ is the matrix with columns the vectors $(1, 0, \ldots, 0)$, $(0, 1, 0, \ldots, 0), \ldots, (0, 0, \ldots, 1)$, i.e.,

$$\mathbf{Z}(0) = \mathbf{I}_{2N}. \tag{16}$$

Later on we are interested in investigating the variational equations when $\mathbf{x}(t; \mathbf{s})$ is a periodic orbit with period T. In this case, the linear equations (10) have periodic coefficients, and the fundamental matrix at $t = T$,

$$\mathbf{M} = \mathbf{Z}(T) = \frac{\partial \mathbf{x}(T; \mathbf{s})}{\partial \mathbf{s}}, \tag{17}$$

is named the *monodromy matrix.* As we shall see, the monodromy matrix plays an important role in the theory of periodic orbits and their stability.

A systematic search of the phase space structure is obtained by locating the following geometrical objects with increasing dimensionality, d.

(1) Stationary (or equilibrium or critical) points, $d = 0$.
(2) Periodic orbits, $d = 1$, and for unstable periodic orbits their stable and unstable manifolds.
(3) Reduced dimension tori, $d < N$, and
(4) KAM tori, $d = N$.

After having located these objects we usually carry out a stability analysis to examine the behaviour of the trajectories in their neighbourhood.

Equilibrium points are those points in phase space for which $\dot{\mathbf{x}} = 0$. To locate them we seek the roots of equation,

$$\nabla H(\mathbf{x}) = 0. \tag{18}$$

The significance of equilibrium points, which coincide with the extrema of the potential energy surface [59], stems from some important theorems which are proved in Milnor's book [60], and state that the topological type of the energy manifolds, $H = E$, changes only at the equilibrium points. Therefore, substantial changes in the dynamics are expected when the total energy exceeds an equilibrium point. The stability of equilibrium points is determined by the second derivatives of the Hamiltonian. Stable equilibrium points, $\mathbf{x}_0$, in the sense of Lyapunov (asymptotically stable) occur when the Hessian of the Hamiltonian, $\partial^2 H$, is positive definite [59]. In this case the eigenvalues of the matrix $\mathbf{J}\partial^2 H(\mathbf{x}_0)$ are pairs of pure imaginary numbers, $\pm i\mu_k$, $k = 1, \ldots, N$. For saddle points there are real eigenvalues, $\pm \mu$, and the corresponding eigenvectors point to the unstable directions.

What happens in phase space as we move away from a stationary point and introduce a small perturbation? For stable equilibrium points the theorems of Kolmogorov–Arnold–Moser (KAM) [14], and of Poincaré–Birkoff (PB) [61] provide an answer. For incommensurable unperturbed frequencies (i.e. there is no relation, $\Sigma_i^N n_i \omega_i = 0$, among the frequencies ω_i and the integers n_i) the KAM theorem guarantees the existence of tori when a small perturbation is introduced, whereas the PB theorem states that the commensurable unperturbed tori will break and an even number of periodic orbits will appear; half of them are stable and half are unstable. By stable we mean that nearby trajectories stay close to the periodic orbit for infinite time, and by unstable we describe the property of nearby trajectories to deviate from the periodic orbit either exponentially or with a power of time t.

After having located the equilibrium points the next geometrical objects of importance are the *periodic orbits*, i.e. those trajectories which close in phase space;

$$\mathbf{x}(T) - \mathbf{x}(0) = 0. \tag{19}$$

One important existence theorem of periodic orbits is that of Weinstein [62]. This theorem guarantees, that arbitrarily close to a stable equilibrium point there are at least N periodic orbits whose periods are close to those of the linearized system. Generalizations of this theorem were given by Moser [63]. A survey of the existence theorems of periodic orbits for nonlinear dynamical systems may be found in [64, 65].

Around stable periodic orbits there are tori which may occupy a significant part of phase space or a very small region. These tori have similar morphology to the periodic
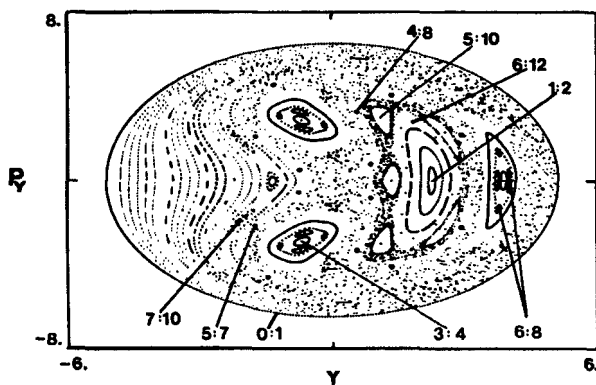
Figure 1. Poincaré surface of section for several trajectories on the plane (y, p_y), and for $x = 0$ and $p_x > 0$. All trajectories correspond to the energy of about 21 atomic units [69].

orbit. Unstable periodic orbits are surrounded by chaotic trajectories or reduced dimension tori (for systems with more than two degrees of freedom). Associated with one unstable periodic orbit are the stable and unstable manifolds which define the separatrix of a resonance. The transport of trajectories from in and out a resonance zone has been discussed by MacKay, Meiss and Percival [66, 67], and Bensimon and Kadanoff [68].

To summarize, the typical structure of phase space at energies where quasi-periodic and chaotic trajectories coexist is as islands of stability surrounded by chaotic seas. Figure 1 shows a typical Poincaré surface of sections obtained with a two-dimensional galactic model potential [69]. The numbers describe the ratio of the two vibrational frequencies (resonance condition) and the lines indicate the position of the intersection of the periodic orbits with the plane of section. Tori, whose intersection with the Poincaré plane are closed smooth curves, surround stable periodic orbits, whereas chaotic trajectories surround unstable periodic orbits. For a chaotic trajectory to move from one resonance region to another, it has to pass through separatrices and that results in the trapping of the trajectory in some regions of phase space (see for example the region around the 5 : 10 resonance in figure 1). Thus, we conclude that periodic orbits at every energy E provide the skeleton of phase space.

3. Phase space structure and spectroscopy

A plethora of numerical results show that the eigenfunctions trace the structure of phase space by staying localized along unstable periodic orbits or in the resonance region of stable periodic orbits [70, 71]. Even examples where eigenfuctions are influenced by the stable and unstable manifolds of unstable periodic orbits have been reported [72]. We have compared time independent and time dependent quantum mechanical calculations with classical results of two model systems and confirmed the above conclusions [69, 73]. In these studies we could classify all calculated eigenfunctions according to the morphologies of the periodic orbits.

Based on these findings, in this section we show how from the phase space structure analysis we can construct spectra pertinent to specific regions of phase space with quantum and classical calculation. Before proceeding to this, we first show how Gutzwiller's semiclassical theory connects periodic orbits, and thus structures of phase space, with vibrational spectra.

3.1. The semiclassical trace formula

The fluctuating part, $N(E)$, of the density of states is predicted by Gutzwiller's trace formula [7] to be,

$$D(E) = \sum_n \delta(E - E_n) = D_{av}(E) + N(E),$$

where

$$N(E) = \text{Re} \sum_{po} \frac{T_{po}}{\pi\hbar} \sum_{j=1}^{\infty} \frac{\exp\left[ij(S_{po}/\hbar - \mu_{po}\pi/2)\right]}{\left[\det(\mathbf{M}_{po}^j - 1)\right]^{1/2}}. \tag{20}$$

$D(E)$ is the density of states at energy E, and $D_{av}(E)$ the average density of states. The sums in equation (20) are over all periodic orbits with period T_{po}, action S_{po}, and for an infinite number of loops j. μ_{po} is the Maslov index (number of turning points) and $\mathbf{M}_{po}^j$ is the stability matrix which describes the results of the transverse displacements off the periodic orbit after j loops. The determinant in equation (20) is evaluated from the eigenvalues of the monodromy matrix,

$$\det(\mathbf{M}_{po}^j - 1) = \prod_{i=1}^{2(N-1)} [\lambda_{po}^j(i) - 1], \tag{21}$$

where $\lambda_{po}^j(i)$ is the jth power of the ith eigenvalue (a complex or real number) of the monodromy matrix which corresponds to a perpendicular direction of the periodic orbit. All the above quantities are computed as functions of the total energy during the periodic orbit analysis.

Generalizations of the trace formula have been given [22, 25], and Miller [23] has proved a relation for semiclassically quantizing specific stable periodic orbits.

According to equation (20) the calculation of the density of states requires a summation over all periodic orbits and for an infinite number of loops of each periodic orbit. This, of course, is impossible for real systems, and therefore there are convergence problems with this equation. However, applications of the trace formula such as in the hydrogen atom in strong magnetic fields [31] have shown that satisfactory results may be obtained by a finite number of periodic orbits. Although accurate eigenvalues are difficult to achieve, low resolution characteristics of the spectra can be identified, and thus, a connection of particular periodic orbits with spectral peaks can be made [74].

3.2. Time dependent quantum calculations: The PO-TDSE method

An immediate association of the periodic orbits and the phase space region around them with the quantum dynamics of the molecule is established by putting an initial wavepacket centred on the periodic orbit and then solving the time dependent Schrödinger equation. Heller [35] has extensively used the time dependent formalism to describe molecular spectra.

The time evolution of the initial wavepacket is followed by solving the time dependent Schrödinger equation;

$$i\hbar \frac{\partial|\phi(\mathbf{q}, t)\rangle}{\partial t} = \hat{H}|\phi(\mathbf{q}, t)\rangle. \tag{22}$$

Several schemes have been proposed for the propagation of the wavepacket $|\phi\rangle$ in time, [75]: (i) second-order difference method, (ii) the split operator algorithm, (iii) representation of the propagator operator in Chebyshev series, and (iv) the Lanczos method.

The spectrum is calculated by first evaluating the time autocorrelation function;

$$C(t) = \langle \phi(\mathbf{q}, 0) | \phi \mathbf{q}, t \rangle, \tag{23}$$

and then computing its Fourier transform,

$$I(E) = \frac{1}{2\pi\hbar} \int_{-\infty}^{\infty} \exp{(iEt/\hbar)} \, C(t) \, dt. \tag{24}$$

The bracket ($\langle \ \rangle$) means integration over the coordinates $\mathbf{q}$.

To see how the eigenvalues are extracted from equation (24), we expand $|\phi(\mathbf{q}, t)\rangle$ as a series of the eigenfunctions $|n\rangle$ of the Hamiltonian $\hat{H}$.

$$|\phi(\mathbf{q}, t)\rangle = \exp{(-i\hat{H}t/\hbar)}|\phi(\mathbf{q}, 0)\rangle = \sum_n \exp{(-iE_n t/\hbar)} |n\rangle\langle n|\phi(\mathbf{q}, 0)\rangle. \tag{25}$$

By introducing the overlap integral, $c_n = \langle n|\phi(\mathbf{q}, 0)\rangle$, the spectrum becomes,

$$
\begin{aligned}
I(E) &= \frac{1}{2\pi\hbar} \sum_n |c_n|^2 \int_{-\infty}^{\infty} \exp{[-i(E_n - E)t/\hbar]} \, dt \\
&= \frac{1}{2\pi\hbar} \sum_n |c_n|^2 \lim_{T \to \infty} \int_{-T}^{T} \exp{[-i(E_n - E)t/\hbar]} \, dt \\
&= \frac{1}{2\pi} \sum_n |c_n|^2 \lim_{T \to \infty} \frac{2\sin{[(E_n - E)T/\hbar]}}{E_n - E} = \sum_n |c_n|^2 \delta(E_n - E).
\end{aligned}
\tag{26}
$$

Thus, for infinite integration time (absolute resolution) we have a sum of delta functions located at the eigenvalues E_n. Finite integration in time (low resolution) will give a sum of broadened peaks which cover several E_n.

We could also extract the eigenfunctions $|n\rangle$ by computing the Fourier transform [76–78],

$$|n\rangle = \frac{1}{c_n} \int_{-\infty}^{\infty} \exp{(iE_n t/\hbar)} |\phi(\mathbf{q}, t)\rangle \, dt. \tag{27}$$

It is clear, that in a time dependent calculation, we locate those eigenfunctions which overlap significantly with the initial wavefunction $|\phi(\mathbf{q}, 0)\rangle$. Since we expect localization of the eigenfunctions around periodic orbits, we simulate the spectrum by taking the appropriate initial wavepacket centred at the place of interest. It can be either an experimental spectrum or a theoretical one, which will reveal those states that are localized at particular regions of phase space. We refer to this method as the periodic orbit-time dependent Schrödinger equation (PO-TDSE).

Taylor and co-workers obtained low-resolution spectra for the hydrogen atom in a magnetic field [79], and the H_3^+ [80], by distributing a basis set of Gaussian functions along the periodic orbit and its neighbourhood. The diagonalization of the Hamiltonian matrix in association with stabilization techniques [81] revealed the eigenfunctions localized in the region of periodic orbit. A direct solution of the time-dependent Schrödinger equation with grid methods [82] is robust and has become more popular in the last few years.

3.3. *Classical calculations*

Although quantum mechanical calculations are always what we should ask, they are not feasible at present for more than three degrees of freedom systems. It is useful

then, to find the classical analogue of the quantum spectrum. In this case, the correspondence between spectrum and phase space structure is more straightforward.

The following formulation has been used in the past [83, 70]. By taking the square of the absolute value of the correlation function $C(t)$, (*the survival probability function*),

$$|C(t)|^2 = |\langle\phi(\mathbf{q}, 0)|\phi(\mathbf{q}, t)\rangle|^2 = \langle\phi(\mathbf{q}, 0)|\phi(\mathbf{q}, t)\rangle\langle\phi(\mathbf{q}, t)|\phi(\mathbf{q}, 0)\rangle, \qquad (28)$$

and using the identity relation,

$$\hat{1} = \sum_n |n\rangle\langle n| \qquad (29)$$

we get,

$$|C(t)|^2 = \langle\phi(\mathbf{q}, 0)|\phi(\mathbf{q}, t)\rangle\langle\phi(\mathbf{q}, t)|\hat{1}|\phi(\mathbf{q}, 0)\rangle$$
$$= \sum_n [\langle n|\phi(\mathbf{q}, 0)\rangle\langle\phi(\mathbf{q}, 0)|\phi(\mathbf{q}, t)\rangle\langle\phi(\mathbf{q}, t)|n\rangle] = \mathrm{tr}\,[\hat{\rho}(0)\hat{\rho}(t)]. \qquad (30)$$

$\hat{\rho}(0)$ is a density operator,

$$\hat{\rho}(0) = |\phi(\mathbf{q}, 0)\rangle\langle\phi(\mathbf{q}, 0)|$$

and

$$\hat{\rho}(t) = |\phi(\mathbf{q}, t)\rangle\langle\phi(\mathbf{q}, t)| = \exp(-i\hat{H}t/\hbar)|\phi(\mathbf{q}, 0)\rangle\langle\phi(\mathbf{q}, 0)|\exp(i\hat{H}t/\hbar), \qquad (31)$$

is the Heisenberg representation of $\hat{\rho}(0)$.

We can pass to the classical analogue by replacing the trace in equation (30) with an integral over the phase space, and by replacing the density operators with classical distribution functions,

$$\Omega(t) = \int \rho[\mathbf{q}(0), \mathbf{p}(0)]\rho[\mathbf{q}(t), \mathbf{p}(t)]\,\mathrm{d}\mathbf{q}\,\mathrm{d}\mathbf{p}. \qquad (32)$$

The classical initial distribution $\rho(0)$ is usually a Wigner or a Husimi transform of the initial quantum wavefunction, $|\phi(\mathbf{q}, 0)\rangle$, [84, 85]. The spectrum is then defined as the Fourier transform,

$$I_c(\omega) = \int \exp(i\omega t)\,\Omega(t)\,\mathrm{d}t. \qquad (33)$$

The classical survival probability function, equation (32), and its Fourier transform, have successfully been used and advanced by Gomez Llorente, Pollak, and Taylor [45, 86].

4. Periodic orbits, stability and continuation/bifurcation diagrams

Stationary points and periodic orbits are the most important classical objects and their knowledge reveals significant information for the dynamics of molecular systems. It is therefore valuable to have methods for locating periodic orbits in conservative Hamiltonian systems of many degrees of freedom such as molecules, which quite often show extreme instabilities. In the following subsection we review such methods. Although we concentrate on periodic orbits the same techniques can be used for locating stationary points on the pes, since stationary points can be considered as the limiting case of zero period, $T \to 0$. We do not review methods for following reaction paths on the pes.

4.1. *Methods for locating periodic orbits*

In order to classify the methods of finding periodic orbits it is appropriate to see this problem as a *two-point boundary value problem*. The boundary conditions are the relations of closing the trajectory in phase space, equation (19).

There are two classes of numerical methods for solving in general two-point boundary value problems [87]. The first class is the *shooting methods* in which the two-point boundary value problem is converted to an *initial value* one. Choosing an initial value for the trajectory we integrate the equations of motion and check the discrepancy in the boundary conditions. By varying the initial conditions or some free parameters we successfully approach the trajectory which satisfies the boundary conditions.

The second class includes the *relaxation methods*. In these methods the differential equations are replaced by difference equations and an appropriate mesh of points for the variables are chosen. Then, starting with an approximate solution we try to bring it into successively closer agreement with the finite difference equations, and with the boundary conditions. Relaxation methods are recommended for unstable systems [87].

Both techniques have been applied to locate periodic orbits in molecules. The shooting methods are the most popular [88]. There are several variants of it [89] which result from fixing the total energy or the period of the periodic orbit, that may or may not use a Poincaré surface of section, and use analytical second derivatives of the Hamiltonian or numerically estimate the gradient in the Newton–Raphson method by integrating neighbouring trajectories. The *monodromy method* of Baranger and co-workers [90–92] is a technique which is classified in the relaxation methods.

An extension of the shooting techniques which tries to incorporate the benefits of the relaxation technique is the *multishooting method* [93–98]. In this case the one-point initial value problem is converted to $(m - 1)$ initial value problems by choosing m nodes in the independent variable. We do not take a finite difference representation of the equations of motion but instead, we integrate $(m - 1)$ trajectories and by varying their $(m - 1)$ initial conditions we approach a smooth trajectory which satisfies the boundary conditions. In the following we describe the multishooting technique.

The boundary value problem is converted to an *initial value problem* by considering the initial values of the coordinates and momenta **s**

$$\mathbf{x}(0) = \mathbf{s}, \tag{34}$$

as independent variables in the nonlinear functions

$$\mathbf{B}(\mathbf{s}) = \mathbf{x}(T; \mathbf{s}) - \mathbf{s}. \tag{35}$$

We denote the roots of equation (35) as $\mathbf{s}_*$, i.e.

$$\mathbf{B}(\mathbf{s}_*) = 0. \tag{36}$$

Thus, if **s** is a nearby value to the solution $\mathbf{s}_*$ we can compute the functions $\mathbf{B}(\mathbf{s})$ by integrating Hamilton's equations for the period T. By appropriately modifying the initial values **s** we hope to converge to the solution, that is $\mathbf{s} \to \mathbf{s}_*$ and $B \to 0$.

The roots of equation (36) are found by a Newton–Raphson method.† The

---

† The Newton–Raphson method is recommended for systems with less than 100 degrees of freedom. For systems with a large number of degrees of freedom, methods such as the conjugate gradient and the variable metric are more suitable [99].

Newton–Raphson method is an iterative scheme and at each iteration, k, we update the initial conditions of the orbit

$$\mathbf{s}_{k+1} = \mathbf{s}_k + \Delta\mathbf{s}_k. \tag{37}$$

The corrections $\Delta\mathbf{s}_k$ are obtained by expanding equation (35) in a Taylor series up to the first order, and then, we solve the linear algebraic equations

$$[\mathbf{Z}_k(T) - \mathbf{I}_{2N}]\Delta\mathbf{s}_k = -\mathbf{B}(\mathbf{s}_k). \tag{38}$$

$\mathbf{Z}_k(T)$ is the fundamental matrix.

Quite often the Newton–Raphson method diverges, although, when it converges it does that quadratically. Sometimes problems of divergencies are cured by scaling the corrections with a parameter λ_k

$$\mathbf{s}_{k+1} = \mathbf{s}_k + \lambda_k\Delta\mathbf{s}_k, \tag{39}$$

where $0 < \lambda_k \leqslant 1$, and $\lambda_k \to 1$ as $\mathbf{s}_k \to \mathbf{s}_*$. These techniques have been named *underrelaxed or damped* Newton–Raphson methods. Several schemes for selecting λ_k have been proposed [94]. A simple one is

$$\lambda_k = \frac{\lambda_{\min}}{\max(\lambda_{\min}, \|\Delta\mathbf{s}_k\|)}. \tag{40}$$

$\lambda_{\min}$ is an input minimum value for the parameter, and $\| \|$ denotes the Euclidean norm of the vector.

The linear system of equations (38), $\Delta\mathbf{s}_k$, may be solved by several algorithms; (i) LU-decomposition methods, (ii) SVD (singular value decomposition) and (iii) iterative methods such as the conjugate gradient, variable metric, and quasi-Newton methods [87].

The idea of multishooting is to combine shooting and relaxation techniques. Let us assume that we divide the period T in $(m-1)$ time intervals, while first for convenience we introduce a new scaled time $\tau = t/T$, $(0 \leqslant \tau \leqslant 1)$,

$$0 = \tau_1 < \tau_2 < \ldots < \tau_{m-1} < \tau_m = 1. \tag{41}$$

Thus, for the simple shooting method $m = 2$.

From now on we drop the index for the iterations k, and we use the index j to denote the nodes in the periodic orbit. If the initial conditions of the trajectory at each node j is $\mathbf{s}_j$ at time τ_j, and the final value of the trajectory at time τ_{j+1} is denoted by $\mathbf{x}(\tau_{j+1}; \mathbf{s}_j)$, then, $(m-2)$ *continuity conditions* should be satisfied (for an illustration see figure 2)

$$\mathbf{C}_j(\mathbf{s}_j, \mathbf{s}_{j+1}) = \mathbf{x}(\tau_{j+1}; \mathbf{s}_j) - \mathbf{s}_{j+1} = 0, \quad j = 1, 2, \ldots, m-2, \tag{42}$$

together with the boundary conditions

$$\mathbf{B}(\mathbf{s}_{m-1}, \mathbf{s}_1) = \mathbf{x}(\tau_m; \mathbf{s}_{m-1}) - \mathbf{s}_1 = 0. \tag{43}$$

Now we have to solve $(m-1)$ initial value problems, and we use again the Newton–Raphson method

$$\mathbf{C}_j(\mathbf{s}_j, \mathbf{s}_{j+1}) + \frac{\partial\mathbf{C}}{\partial\mathbf{s}_j}\Delta\mathbf{s}_j + \frac{\partial\mathbf{C}}{\partial\mathbf{s}_{j+1}}\Delta\mathbf{s}_{j+1} = 0, \tag{44}$$

which become

$$\mathbf{C}_j(\mathbf{s}_j, \mathbf{s}_{j+1}) + \mathbf{Z}_j(\tau_{j+1})\Delta\mathbf{s}_j - \Delta\mathbf{s}_{j+1} = 0, \quad 1 \leqslant j \leqslant m-2. \tag{45}$$
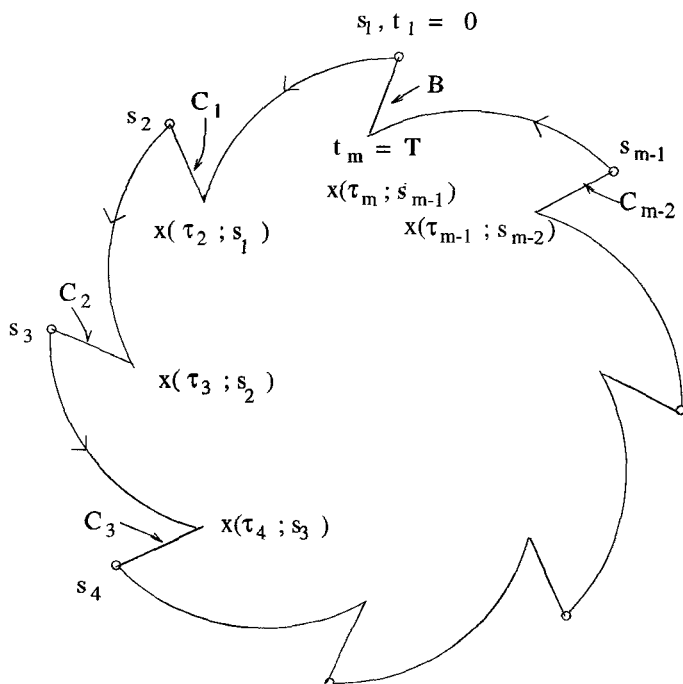
Figure 2.   A schematic representation of the multishooting method for locating periodic orbits.

Using the boundary conditions (equation (43)) we get

$$\mathbf{B}(\mathbf{s}_{m-1}, \mathbf{s}_1) + \mathbf{Z}_{m-1}(\tau_m)\Delta\mathbf{s}_{m-1} - \Delta\mathbf{s}_1 = 0, \tag{46}$$

where,

$$\mathbf{Z}_j(\tau_{j+1}) = \frac{\partial\mathbf{x}(\tau_{j+1}; \mathbf{s}_j)}{\partial\mathbf{s}_j}. \tag{47}$$

Equations (45, 46) are written in a matrix form of dimension $2N(m-1) \times 2N(m-1)$

$$\begin{bmatrix} \mathbf{Z}_1 & -\mathbf{I}_{2N} & 0 & \dots & 0 & 0 \\ 0 & \mathbf{Z}_2 & -\mathbf{I}_{2N} & \dots & 0 & 0 \\ \dots & \dots & \dots & \dots & \dots & \dots \\ 0 & 0 & 0 & \dots & \mathbf{Z}_{m-2} & -\mathbf{I}_{2N} \\ -\mathbf{I}_{2N} & 0 & 0 & \dots & 0 & \mathbf{Z}_{m-1} \end{bmatrix} \begin{bmatrix} \Delta\mathbf{s}_1 \\ \Delta\mathbf{s}_2 \\ \dots \\ \Delta\mathbf{s}_{m-2} \\ \Delta\mathbf{s}_{m-1} \end{bmatrix} = - \begin{bmatrix} \mathbf{C}_1 \\ \mathbf{C}_2 \\ \dots \\ \mathbf{C}_{m-2} \\ \mathbf{B} \end{bmatrix} \tag{48}$$

The above system of linear equations is solved by invoking the so called *condensing algorithm* [95]

$$\Delta\mathbf{s}_1 = -\mathbf{E}^{-1}\mathbf{u}, \tag{49}$$

$$\Delta\mathbf{s}_{j+1} = \mathbf{Z}_j\Delta\mathbf{s}_j + \mathbf{C}_j, \quad j = 1, 2, \dots, m-2, \tag{50}$$

where

$$\left.\begin{array}{l} \mathbf{E} = \mathbf{Z}_{m-1}\mathbf{Z}_{m-2} \dots \mathbf{Z}_2\mathbf{Z}_1 - \mathbf{I}_{2N}, \\ \mathbf{u} = \mathbf{B} + \mathbf{Z}_{m-1}(\mathbf{C}_{m-2} + \mathbf{Z}_{m-2}(\mathbf{C}_{m-3} + \mathbf{Z}_{m-3}(\mathbf{C}_{m-4} + \dots + \mathbf{Z}_2\mathbf{C}_1) \dots)). \end{array}\right\} \quad (51)$$

The $(m-1)$ fundamental matrices required in the multishooting method are evaluated either from numerically obtained derivatives or analytically. The first requires the integration of $2N(m-1)$ neighbouring trajectories, and the derivatives are then computed by finite differences. In the case that the analytic second derivatives of the Hamiltonian are available, we integrate Hamilton's and variational equations (equations (10)) together. After converging to the periodic orbit we can have an estimate of the monodromy matrix from the product of matrices

$$\mathbf{M} = \mathbf{Z}_{m-1}\mathbf{Z}_{m-2} \dots \mathbf{Z}_2\mathbf{Z}_1. \quad (52)$$

Sometimes it is desirable to bring all periodic orbits on a common Poincaré surface of section. The Henón method [100] is not suitable for highly unstable systems. Then, it is more convenient to increase the boundary conditions by fixing one coordinate (momentum), i.e.,

$$x_l - \xi = 0, \quad (53)$$

and to consider, that the period of the periodic orbit satisfies the trivial differential equation [97]

$$\dot{T} = 0. \quad (54)$$

Thus, a $(2N+1)$ dimensional boundary value problem must be solved.

4.2. Stability of periodic orbits

The behaviour of the nearby trajectories to the periodic orbit is examined by studying the eigenvalues of the monodromy matrix λ_i. Sometimes it is convenient to express the eigenvalues of the monodromy matrix as,

$$\lambda = \exp(\alpha T), \quad (55)$$

where the exponents α are called *characteristic exponents*.

From the general solution of variational equations (equation (11)) we deduce

$$\boldsymbol{\zeta}(nT) = \mathbf{M}(T)^n\boldsymbol{\zeta}(0) = \begin{pmatrix} \lambda_1^n & 0 & \dots & 0 \\ 0 & \lambda_2^n & \dots & 0 \\ \dots & \dots & \dots & \dots \\ 0 & 0 & \dots & \lambda_{2N}^n \end{pmatrix} \boldsymbol{\zeta}(0), \quad (56)$$

assuming that the coordinate system is the set of the eigenvectors of $\mathbf{M}$. Obviously, the eigenvalues of the monodromy matrix describe the deviation from the periodic orbit of an initial displacement $\boldsymbol{\zeta}(0)$ after n iterations.

From the symplectic properties of the Hamiltonian systems we know that the eigenvalues of the monodromy matrix always appear in pairs; either complex conjugate or inverse real numbers. Also, because of the conservation of the total energy two eigenvalues are always equal to one. Thus, excluding the two unit eigenvalues the following cases can arise [101]:

(i) If all the eigenvalues are on the unit complex circle, and multiple eigenvalues

have independent eigenvectors which are equal to the multiplicity of the eigenvalues, then, the periodic orbit is *stable* (*elliptic*), and it is surrounded by tori. The characteristic exponents are pure imaginary numbers and maybe considered as the frequencies of rotation of a neighbouring trajectory around the periodic orbit, $\alpha = i\sigma$.

It may happen that,

$$T/(2\pi/\sigma) = m/n, \tag{57}$$

where m, and n are integers. Then, it can be shown that the variational equations have a periodic solution, and there should be a new periodic orbit of period $T' = nT$ in the neighbourhood of the initial one.

(ii) If there are eigenvalues equal to one, then $\alpha = 0$ and a new periodic orbit of period T also exists in the neighbourhood of the parent one. For eigenvalues equal to -1, $\alpha = i\pi/T$ and a new periodic orbit of double period exists nearby.

(iii) If there are real eigenvalues greater than ± 1, $\zeta(t)$ will deviate exponentially with time, and the periodic orbit is *unstable* (*hyperbolic*) in the directions of the corresponding eigenvectors.

(iv) If there is a complex eigenvalue, λ, with norm greater than one, then λ^{-1}, $\lambda*$, and $(\lambda*)^{-1}$ are also eigenvalues, and the periodic orbit is called *complex unstable*.

(v) If there are multiple eigenvalues with independent eigenvectors less than the multiplicity of the eigenvalue, the periodic orbit is unstable with $\zeta(t)$ deviating not exponentially but with a power of t.

In figure 3 we plot the eigenvalues of $\mathbf{M}$ on the unit complex circle for a system of three degrees of freedom. The two pairs of eigenvalues which are different than one may be: complex conjugate with norm equal to one (stable orbits), or one pair of complex conjugate with unit norm and one pair of real eigenvalues (single unstable
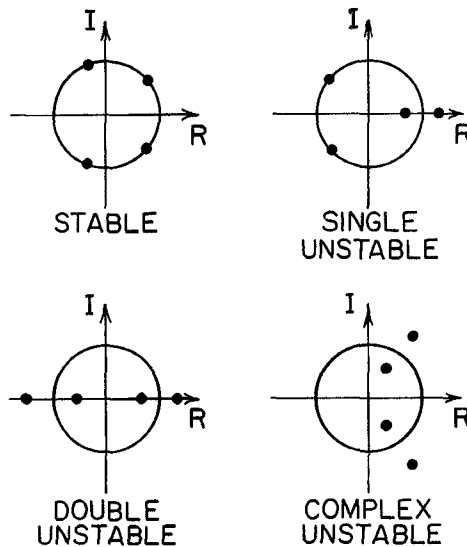

Figure 3. A schematic representation of the types of instabilities of periodic orbits in a 3D Hamiltonian system. The dots denote the eigenvalues of the monodromy matrix.

periodic orbits), or two real pairs for double unstable periodic orbits. There are three different cases in the double instability; positive, negative, or one positive and one negative pairs of real eigenvalues. Finally, if there is a quadruplet of complex eigenvalues the periodic orbit is complex unstable [102].

In a recent article [103], we have addressed the question of the classical–quantum correspondence in the case of complex instability. Remarkable agreement was found in the dynamical behaviour of a 3D model system.

For polyatomic molecules with more than three degrees of freedom the same kinds of instabilities appear, but with more combinations. For example, in a tetratomic molecule, such as acetylene [104], we find double complex instability.

4.3. *Continuation/bifurcation diagrams*

In investigating the phase space structure of a molecule it is important to follow the evolution of a family of periodic orbits with respect to the total energy. Then, the question about the change of stability of periodic orbits and the possibility of finding new families of periodic orbits arises. Specifically, we can ask when a stable periodic orbit will become unstable by varying a parameter of the Hamiltonian. The answer to this problem is given by the theory of Krein, Gelfand, and Lindskii [105, 101].

For a system of two degrees of freedom with only one pair of eigenvalues moving on the unit complex circle by varying the total energy of the system, the eigenvalues come out on the real axis at ± 1. In this case, bifurcation of new families of periodic orbits are observed with the same period as that of the parent periodic orbit, when the collision of the eigenvalues happens at 1. When the eigenvalues collide at -1 the new periodic orbits are of double period. In the latter case the parent periodic orbit becomes unstable and is often called *hyperbolic by reflection*. For three and higher degrees of freedom systems several combinations may happen as is explained in figure 3.

Can we predict the number and the stability of the bifurcating families of periodic orbits? The answer to this question is given by *degree theory* [106]. The basic concept in this theory is the conservation of *rotation*.

Plots of the initial coordinates or momenta of the periodic orbits as functions of the varying parameter (in our case the total energy or the period) are named *continuation* or *bifurcation diagrams*, and show the continuation of the family of periodic orbits with the parameter as well as the critical values of the energy for bifurcation. Usually, we plot projections of these diagrams on several planes, and as we shall see, the continuation diagrams reveal the structure of phase space.

In figure 4 we show several bifurcation schemes which are frequently encountered in Hamiltonian conservative systems. The continuous lines represent stable orbits and the dashed lines unstable ones. One important type of bifurcation is the *saddle-node*. It appears in the *neighbourhood* of tangencies of the stable and unstable manifolds of an unstable periodic orbit according to Newhouse theorems [107, 108]. Numerical examples of such tangencies have been given [109, 110]. We can see from figure 4 that a saddle-node bifurcation point is the coalescence of the stable and unstable periodic orbit. Since saddle-node bifurcations may occur at high excitation energies, the stable periodic orbits create stability islands even in highly chaotic regions of phase space. This has significant implications for molecular systems.

In the continuation of a family of periodic orbits we use predictor–corrector algorithms with trivial or secant predictors and a Newton–Raphson corrector [111–113].
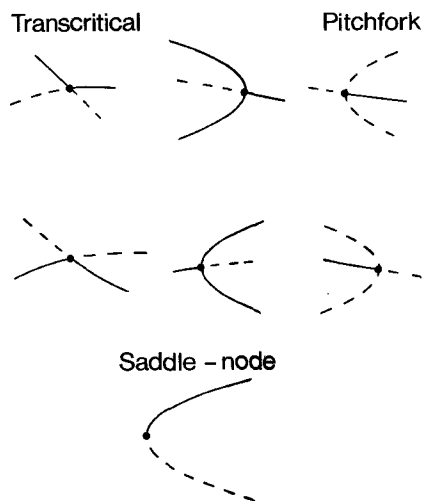
Figure 4. Bifurcation schemes of families of periodic orbits with respect to the varying parameter. Continuous lines represent stable orbits, dashed lines unstable orbits.

5. Applications

5.1. *Triatomic molecules*

Molecular potential energy surfaces are calculated in the Born–Oppenheimer approximation and they are described by analytical functions [114]. To be useful in dynamical calculations, pes must give a global description of the nuclear configuration space, and usually they have more than one minima. It is however common, mainly in spectroscopic studies, to obtain pes which give a local description of the minimum.

According to the methodology developed in the previous sections, given a pes we first find the minima and the saddle points. For a small polyatomic molecule this is not difficult, since a few stationary points are supported by the potential function. However, for large clusters the location of stationary points may become the main task. The techniques used to locate periodic orbits may also be used for stationary points, since they can be considered as the limiting case of zero period. Special methods are needed to find reaction paths. Recent work on water clusters demonstrates our methods to find stationary points and their association to the dynamic and thermodynamic properties of the clusters [115–118].

For small polyatomic molecules families of periodic orbits are the most important objects for extracting the dynamics of the molecule. From each minimum of the pes at least N families of periodic orbits emanate according to Weinstein's theorem [62] and we name them *principal* families. Each principal family corresponds to a vibrational normal mode of the molecule. By constructing continuation/bifurcation diagrams we can locate bifurcating families from the principal ones.

From a saddle point of the pes with one unstable direction at least $N - 1$ principal families of periodic orbits emanate [63], which in turn, may also give rise to new bifurcating families.

Another interesting type of periodic orbits are those which are generated from saddle-node bifurcations. As we stated before, they emanate from tangencies of the stable and unstable manifolds of unstable periodic orbits [107, 108], and therefore, they may appear at every region of phase space. An important result of our work is the
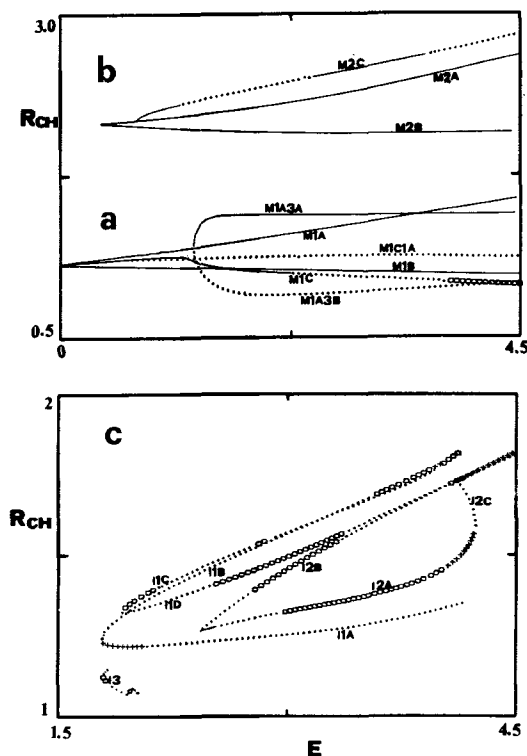
Figure 5.   Continuation diagram of (a) HCN, (b) HNC, and (c) rotating type of periodic orbits
above the potential barrier of isomerization [122].

systematic location of saddle-node bifurcations of periodic orbits above potential
barriers. These periodic orbits usually connect separate minima on the pes and we have
named them earlier as rotating, isomerizing [119], as well as irregular, a term adopted
by astronomers [120].

One of our first studies was hydrogen cyanide [121, 122]. This molecule has been
studied extensively by spectroscopists who predict regular vibrational states with
extended excitations in the stretch modes [46]. A significant number of theoretical
papers have also been published, both classical [123] and quantum mechanical
[121, 124].

The pes of the ground electronic state has two minima, which correspond to the
stable linear molecule, HCN, and to the metastable isomer, HNC, at the energy of
0·484 eV above the absolute minimum. The barrier of isomerization is 1·51 eV.

In figure 5 we show bifurcation diagrams for the families of periodic orbits which
we have located. Those families which emanate from the absolute minimum are denoted
as M1A, M1B, etc. Families emanating from the second minimum are denoted as M2,
whereas the periodic orbits which appear above the barrier of isomerization are denoted
with the prefix I. Solid lines correspond to stable periodic orbits, dotted lines to single
unstable (the monodromy matrix has one pair of real eigenvalues), and the squares to
double unstable (two pairs of real eigenvalues) periodic orbits. Crosses are for complex
unstable periodic orbits, i.e. the monodromy matrix gives one quadruplet of complex
eigenvalues.

From these diagrams we can draw some important conclusions about the dynamical behaviour of the molecule. The motions which describe stretches of CH, and CN (these correspond to the periodic orbits M1A and M1B respectively) remain stable at energies even above the first dissociation limit. This regularity has been confirmed in time dependent quantum mechanical calculations as well [122]. Trajectories associated with excitation of the bend mode (periodic orbits of M1C type) are also regular up to 0·75 eV above the potential barrier of isomerization. States related with the isomerization process are localized along the I type periodic orbits, and they originate from saddle-node bifurcations.

These conclusions are confirmed not only from the quantum mechanical calculations [122, 124], but also from recent SEP spectroscopic experiments [46]. We have also compared the classical survival probability function of HCN with its quantum mechanical analogue [123], and the theoretical classical mechanical spectrum with the experimental dispersed fluorescence results [125].

Producing more accurate potential energy surfaces is highly desirable in molecular dynamics calculations, and it is quite common for new versions of the potential functions to appear constantly. The question how and to what extent the modifications of the pes change the dynamics predicted with the old version of the pes is important. Since continuation diagrams of periodic orbits carry a significant part of the dynamical properties of the molecule, comparison of the continuation diagrams produced from different versions of the potential offer an inexpensive way to evaluate the accuracy of the potential functions. Such a study was carried out for HCN [126] by comparing the bifurcation diagram of the global pes with a local potential function of HCN obtained by Carter *et al.* [127].

Contrary to HCN ozone has been found to be highly unstable in the excited electronic state $^1B_2$. The absorption spectrum $D^1B_2 \leftarrow X^1A_1$, shows a broad peak, the Hartley band [48]. The main interest in this spectrum is a weak structure on the top of Hartley's band, which consists of small peaks separated by approximately $250\,\mathrm{cm}^{-1}$. Johnson and Kinsey [50] produced the survival probability function from the experimental spectrum, and carried out a periodic orbit search. Farantos and Taylor [128] also carried out 3D classical calculations, but found no oscillatory structure in the survival probability function. 3D quantum mechanical correlation functions have also been calculated that show a rich oscillatory structure [129, 130]. No interpretation was given for the dynamics of the molecule.

In order to elucidate these discrepancies we have performed quantum mechanical calculations by solving the time-dependent Schrödinger equation and restricting the problem into two dimensions [77, 131] by freezing the angle between the two bond lengths. Figure 6 shows the 2D quantum survival probability function, which contrary to the classical one, has indeed a very rich structure. By examining snapshots of the evolving wavepacket it was not difficult to understand the origin of the oscillations in the survival probability function. It results from the reflected part of the wavepacket from the potential walls on its way towards the exit channels.

Still, it is difficult to understand the dynamics of the system from these plots. Therefore, we tried to locate the periodic orbits which have the same periods as the recurrence times extracted from the correlation function (figure 7). The period of these periodic orbits or half of it for the symmetric ones, is in accord with the recurrence times found in the quantum time autocorrelation function.

The instability of these periodic orbits is so high that in our first publication [131] it was difficult to close them accurately and to construct continuation diagrams.
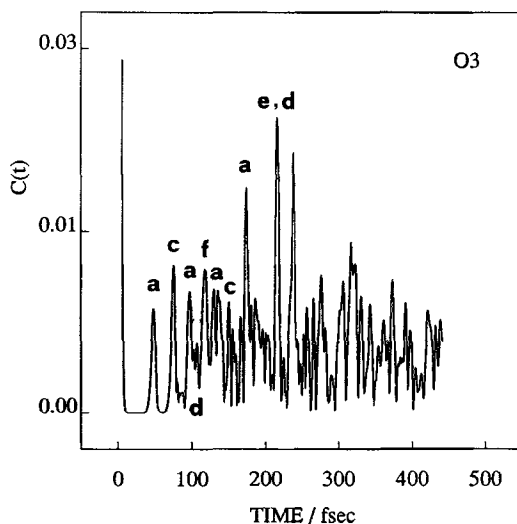
Figure 6. The quantum time autocorrelation function of ozone [77].

Recently, using the multishooting algorithm it was possible to follow them with the energy, and to show that these periodic orbits which emanate above the barrier of dissociation originate from saddle-node bifurcations [132].

It is interesting to mention that periodic orbits of saddle-node type $7c$ and $7d$ were found for CO_2 [133, 134], as well as for the doubly excited helium atom [135, 136].

In conclusion we can state, that for ozone although classical mechanics fails to reproduce the quantum mechanical survival probability function, and this is because of the high instability of the system, however periodic orbits can be used to explain the quantum localization, and to elucidate the detailed dynamics of the system.

SO_2 is an important molecule for atmospheric and combustion chemistry. Furthermore, for some time now, it has also attracted the interest of workers wishing to investigate molecular chaos. Using an empirical potential function for the ground electronic state, Farantos and Murrell [137] found that the onset of chaotic dynamics is at about 1·5 eV above the minimum. Frederick, McClelland, and Brumer [138] showed that even at 1·9 eV a substantial region of phase space is occupied by regular trajectories. Experimental results have recently been obtained by Yamanouchi *et al.* [41, 43], who have studied the vibrational spectroscopy of the ground electronic state of this molecule using dispersed fluorescence (DF), and stimulated emission pumping (SEP) techniques [139].

A periodic orbit analysis has been carried out for the ground [74], and the excited state [77] that is used in the SEP experiment. For the electronically excited state it was shown that saddle-node bifurcations of periodic orbits create extended stable regions in phase space, and regular quantum eigenfunctions are localized on them.

These wavefunctions are used to assign initial conditions to the trajectories run in the ground electronic surface in order to calculate the classical survival probability function.

In figure 8 the bifurcation diagram for the electronic ground state is shown projected in the (E, p_{r2}) plane. From the absolute minimum of the potential the three principal
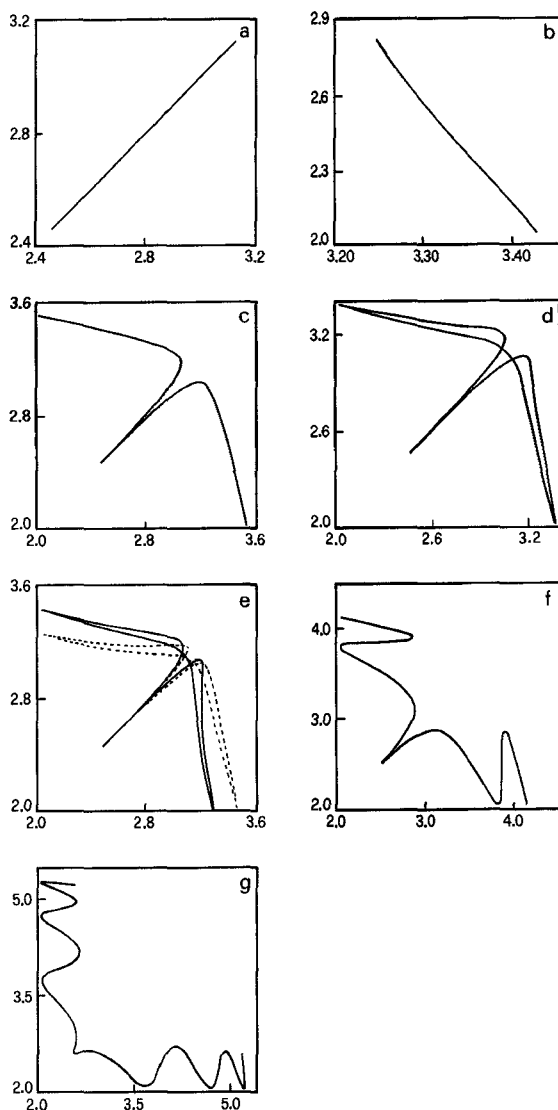
Figure 7. Periodic orbits found in the excited state of ozone [131].

families emanate and they are labelled as SS, AS, and B, and correspond to the symmetric stretch, antisymmetric stretch, and bend modes respectively. Continuous lines mark stable periodic orbits, dotted lines correspond to single unstable periodic orbits, and open circles to double unstable periodic orbits. Families which bifurcate are denoted by numerals, whereas the different branches are labelled with the letters A and B.

We have found a saddle-node bifurcation above the lowest potential barrier of the linearization of the molecule and the stable and unstable families are denoted by R1A, and R1B respectively. These periodic orbits connect the two symmetrically located minima, (OSO), on the potential function.

Figure 9 shows the fluctuating part of the semiclassical density of states using the
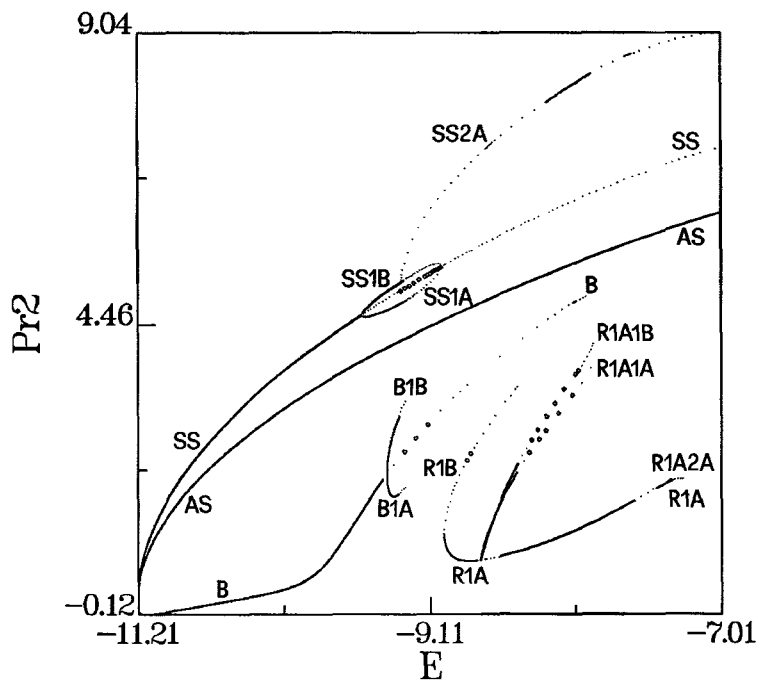
Figure 8.   Bifurcation diagram for the ground electronic state of SO_2. E is the total energy of the molecule and p_{r2} the momentum of one of the SO bond lengths [74].
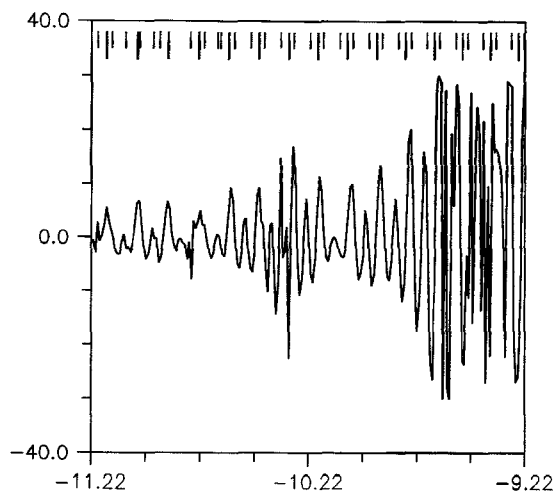

Figure 9.   The fluctuating part of the density of states calculated with Gutzwiller's trace formula and the symmetric stretch (SS) and bend (B) principal families of periodic orbits [74].

symmetric stretch and bend principal families of periodic orbits, SS, and B. The vertical lines at the top of the figure denote the quantum levels assigned by Yamanouchi *et al.* [43]. They are mainly progressions in the symmetric stretch $(v_1, 0, 0)$, $(v_1 = 1-15)$, bend $(0, v_2, 0)$, $(v_2 = 1-5)$ and $(v_1, v_2, 0)$, $(v_2 = 1, 2)$. Spectroscopically, more levels have been located among those which we show.

The bifurcation diagram, classical survival probability functions, and the trace formula confirm the regularity of the spectrum and the preference for exciting the symmetric stretch and bend normal modes in the ground electronic state found by Yamanouchi *et al.* [43].

In an effort to explore the dynamics of molecular systems bound by different types of forces, a periodic orbit analysis was performed for a van der Waals cluster, ArCO [140]. We kept the CO bond length fixed at its equilibrium value, r, and studied the dynamics in the coordinates (R, θ); R is the distance of Ar from the centre of mass of CO, and θ the angle between R, and r. The potential function has one minimum, and two saddle points for linear geometries.

The bifurcation diagram is shown in figure 10. R1 and TH1 denote the principal families which emerge from the minimum, and imply excitation in the stretch and bend modes respectively. Birfurcating families are characterized with the letter A and B; i.e. TH1A, TH1B, R1A etc. Continuous curves correspond to stable periodic orbits, and dotted curves to unstable periodic orbits. Periodic orbits which appear above the barriers of linearization of the molecule are labelled as I. They are of saddle-node type, and occur in pairs, one stable and one unstable.

In order to examine more globally the phase space we draw Poincaré surfaces of section. One is shown in figure 11 at an energy above the first barrier but below the second one $(E = -0.0087 \, \text{eV})$. We can see that the phase space is dominated by chaos, but small islands of stability exist which surround the I1A periodic orbit.

This classical structure has been used to explain the topologies of the quantum eigenfunctions. It has been found [141] that among twenty bound states extended to all available configuration space, four are localized. The zero point energy of ArCO is just above the barrier of linearization of the molecule, where we have seen that the classical chaos dominates. Therefore, the delocalization of the eigenstates is not surprising. On the contrary, the localized ones, which are embedded in the delocalized states, are unexpected and their existence is explained by the saddle-node bifurcations.

Periodic orbits of isomerizing (or rotating) type, i.e. orbits moving across a potential barrier, have been found for other systems as well. Pollak [142] studied the association of hyperspherical periodic orbits and resonances in atom–diatom reactions. Taylor and co-workers used similar types of periodic orbits for the assignment of photodetachment spectra in H_2F [143], and HCl_2 [144]. Gomez and Pollak [145] used isomerizing T-shape periodic orbits to explain regularities in the low-resolution photodissociation spectra of H_3^+, whereas 3D quantum and classical calculations have recently been reported by Tennyson and collaborators [146, 147].

Indications for the existence of saddle-node type periodic orbits in Ar_3 gave the calculation of Lyapunov exponents by Berry and co-workers [148]. They noticed that for energies above the barrier of linearization of argon trimer, the Lyapunov exponents decrease, something which could be anticipated from the existence of saddle-node families of periodic orbits. We have done a periodic orbit analysis on a model potential of Ar_3 and we indeed found such periodic orbits [149].
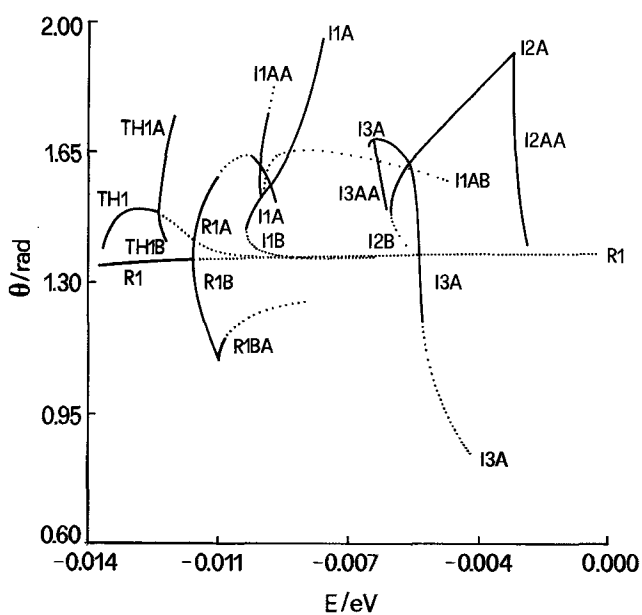
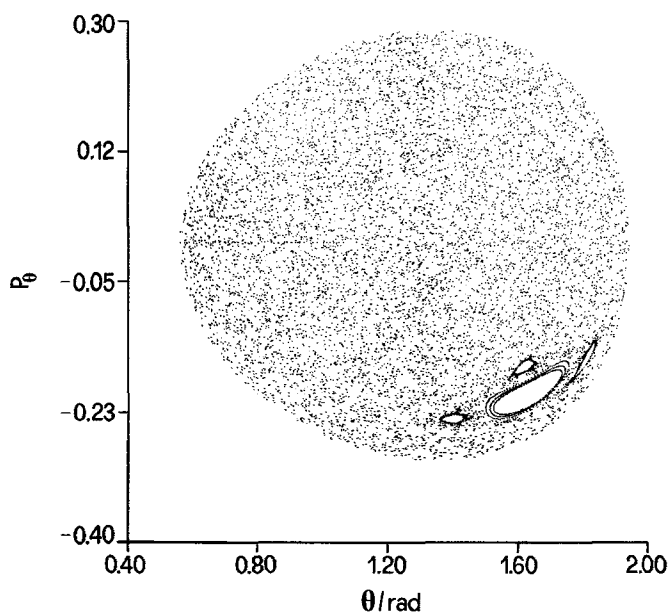Figure 10.   Bifurcation diagram of ArCO van der Waals cluster [140].

Figure 11.   Poincaré surface of section for ArCO at the energy of − 0·0087 eV. The large
stability island is due to the stable periodic orbit that originates from the saddle-node
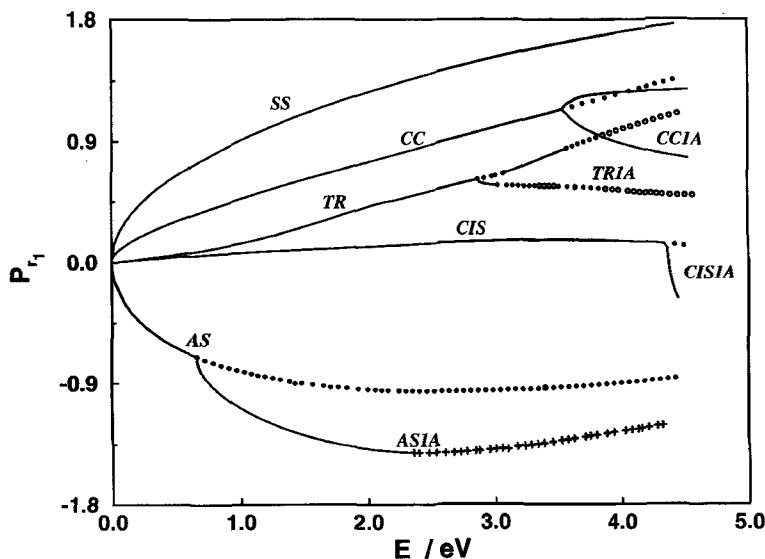bifurcation I1A [140].

Figure 12. Bifurcation diagram of C_2H_2 [104].

5.2. *Tetratomic molecules*

If the periodic orbit analysis and generally the classical mechanical methods are going to be useful in vibrational molecular spectroscopy they have to be tested for polyatomic molecules. Therefore, the extension of the previous techniques has been made to a tetratomic molecule of six degrees of freedom, and acetylene was chosen as a prototype system.

The vibrational spectroscopy of acetylene in the electronic ground state has been studied extensively by Field and collaborators [37, 38]. One of the reasons for that is the association of acetylene with the studies of vibrational chaos. Using dispersed fluorescence (DF) and stimulated emission pumping (SEP) spectroscopy, vibrational spectra have been recorded at low and high resolution covering an energy range up to about $28\,000\,cm^{-1}$. The high-resolution SEP spectra near $27\,900\,cm^{-1}$ revealed levels which satisfy some of the criteria for quantum chaos.

Contrary to that, low-resolution spectra show peaks which can be labelled with approximate quantum numbers related to the normal modes of the molecule. By increasing the resolution each peak is resolved to more peaks which may also be labelled by approximate quantum numbers. The clumps observed in the low-resolution DF spectra have been named by Yamanouchi *et al.* [37] as *feature states*.

We have located the principal families which emanate from the minima of acetylene, vinilydene, and the saddle point that separates the two minima. It was not difficult to construct continuation/bifurcation diagrams and to locate saddle-node bifurcations [104]. Dealing with a 6D system several combinations of the stabilities of periodic orbits are expected. It is interesting to see that the principal periodic orbits remain stable for a substantial range of energies.

Figure 12 shows a projection of the bifurcation diagram in the (E, p_{r1}) plane, that refers to the acetylene minimum. p_{r1} is the momentum conjugate to the distance of hydrogen atom 1 from the centre of mass of CC diatom. We chose this projection since it exposes better the continuation of the families of periodic orbits avoiding intersections

on the projection plane. Each curve corresponds to a family of periodic orbits, and is related with one of the normal modes of the molecule (at least for energies close to the minimum). Thus, we label the principal families of periodic orbits as symmetric stretch (SS), antisymmetric stretch (AS), carbon–carbon stretch (CC), *trans*-bend (TR) and *cis*-bend (CIS).

Each point on a curve denotes the initial conditions of the periodic orbit at energy E, and solid lines mean that the periodic orbits are stable. Dotted lines signal that the stability of periodic orbits has changed to single unstable, that is, the motion in one degree of freedom has become unstable. The open circles mark double unstable orbits, and the crosses complex instability. Once we found one periodic orbit of each family, starting from the minimum of the potential, the construction of the bifurcation diagram was very easy.

The shown bifurcation diagram covers an energy range of 4·5 eV and with the exception of the AS family all other families of periodic orbits are stable for substantial range of energies. The symmetric stretch family (SS) is stable for the whole energy range. The TR family turns to single unstable at 2·9 eV above the minimum, then becomes stable again, and eventually turns to double unstable. The CIS family remains stable for most of the studied energy interval, and the CC family changes stability at 3·6 eV. The bifurcating family, AS1A, from the AS starts stable and with the same period as the parent one, and then turns to complex unstable.

The stable regions in phase space around the periodic orbits are reflected in the regularity of the classical survival probability function. As in the case of SO_2, classical spectra and Gutzwiller's trace formula elucidate the regularities and the assignment of the low-resolution spectra of the molecule [104].

6.   Conclusions

In this article we have reviewed and hopefully demonstrated how periodic orbit theory of dynamical systems can be applied to analyse vibrational spectra of highly energized molecules. Periodic orbit analysis in the way we apply it offers a systematic method to explore the dynamics of the molecule, to obtain vibrational spectra and associate them with the dynamical behaviour of the molecule, and most important, to make predictions about localization effects as the existence of saddle-node type states above potential barriers which we have found in most of the studied cases.

Of course, the questions of how easy is it to locate periodic orbits and to construct a detailed continuation/bifurcation diagram always remain. Our results on C_2H_2 are quite promising [104]. Especially, the multishooting technique for finding periodic orbits is robust and suitable for polyatomic molecules. This method is particularly suited for highly unstable systems [132].

Another problem encountered in polyatomic molecules with a significant number of degrees of freedom is the identification of regions of phase space where spectroscopically important periodic orbits exist. This problem is related to the task of finding good initial conditions for the Newton–Raphson process in locating periodic orbits. The construction of the continuation/bifurcation diagram started from equilibrium points secures the identification of the principal from the bifurcating families. Symmetries in phase space always help to locate periodic orbits and must be used. However, the location of the saddle-node bifurcation is a more difficult task.

We have used the classical survival probability function for exploring particular regions of phase space. We have seen that in unstable regions peaks in the classical

correlation function are due to trajectories which provide good initial conditions for the nearby periodic orbits. We find correlation functions and their Fourier transforms less expensive than calculating local Lyapunov exponents recently proposed by Pollak [89, 150].

The question about the validity and accuracy of the semiclassical and classical theories of vibrational spectra is also quite severe. However, if we take into account that for most polyatomic molecules low-resolution spectra are available, then the good correspondence between classical and quantum dynamics expected for short times, validates the assignment of the spectroscopic features with periodic orbits. Furthermore, we expect for low-resolution spectra the principal families of periodic orbits and short period bifurcations of them to be enough for explaining regularities. For these reasons we believe that the periodic orbit method will remain one of the techniques [34] of analysing molecular vibrational spectra.

References

[1] KARPLUS, M., PORTER, R. N., and SHARMA, R. D., 1965, *J. chem. Phys.*, **43**, 3259.

[2] BAER, M. (editor), 1985, *Theory of Chemical Reaction Dynamics*, Vol. 3 (Boca Raton, FL: CRC).

[3] CASATI, G., GUARNERI, I., and STEPELYANSKY, D. L., 1991, *Chaos, Solitons and Fractals*, **1**, 131.

[4] GERBER, R. B., McCOY, A. B., and GARCIA-VELA, A., 1994, *Ann. Rev. Phys. Chem.*, **45**, 275.

[5] FINCHAM, D., and HEYES, D. M., 1985, *Adv. chem. Phys.*, **63** (New York: Wiley), p. 493.

[6] REINHARDT, W. P., 1984, *The Mathematical Analysis of Physical Systems*, Vol. 3. edited by R. Mickens (New York: Van Nostrand).

[7] GUTZWILLER, M. C., 1990, *Chaos in Classical and Quantum Mechanics* (Berlin: Springer-Verlag).

[8] GUCKENHEIMER, J., and HOLMES, P., 1983, *Nonlinear Oscillations, Dynamical Systems, and Bifurcations of Vector Fields* (Berlin: Springer-Verlag).

[9] SCHECK, F., 1990, *Mechanics, from Newton's Laws to Deterministic Chaos* (Berlin: Springer-Verlag).

[10] FARANTOS, S. C., and TENNYSON, J., 1987, *Stochasticity and Intramolecular Redistribution of Energy*, edited by R. Lefebvre and S. Mukamel (Dordrecht: D. Reidel), p. 15.

[11] MACKAY, R. S., and MIESS, J. D., 1987, *Hamiltonian Dynamical Systems* (Bristol: Adam Hilger).

[12] BERRY, M. V., 1991, *Les Houches Lecture Series*, edited by M.-J. Giannoni and A. Voros, Vol. 52 (Amsterdam: North-Holland), p. 251.

[13] NAKAMURA, K., 1993, *Quantum chaos, a new paradigm of non-linear dynamics*, Cambridge Nonlinear Science Series, Vol. 3 (Cambridge University Press).

[14] ARNOLD, V. I., and AVEZ, A., 1968, *Ergodic Problems of Classical Mechanics* (New York: Benjamin).

[15] BOHIGAS, O., GIANNONI, M.-J., and SCHMIDT, C., 1986, *Quantum Chaos and Statistical Nuclear Physics, Lecture Notes in Physics*, Vol. 263 (Berlin: Springer-Verlag).

[16] McDONALD, S. W., and KAUFMAN, A. N., 1979, *Phys. Rev. Lett.*, **42**, 1189.

[17] HELLER, E. J., 1984, *Phys. Rev. Lett.*, **53**, 1515.

[18] O'CONNOR, P., GEHLEN, J., and HELLER, E. J., 1987, *Phys. Rev. Lett.*, **58**, 1296.

[19] GUTZWILLER, M. C., 1967, *J. math. Phys.*, **8**, 1979.

[20] GUTZWILLER, M. C., 1971, *J. math. Phys.*, **12**, 343.

[21] BALIAN, R., and BLOCH, C., 1974, *Ann. Phys.*, **85**, 514.

[22] BERRY, M. V., and TABOR, M., 1976, *Proc. R. Soc. Lond.* A, **349**, 101.

[23] MILLER, W. H., 1975, *J. chem. Phys.*, **63**, 996.

[24] BOGOMOLNY, W. B., 1988, *Physica* D, **31**, 169.

[25] BOGOMOLNY, W. B., 1992, *Chaos*, **2**, 5.

[26] CVITANOVIĆ, P., 1991, *Physica* D, **51**, 138.

[27] GUTZWILLER, M., 1991, *Chaos and Quantum Physics*, edited by M.-J. Giannoni, A. Voros, and J. Zinn-Justin (Elsevier Science Publishers B.V.), p. 203.

[28] POINCARÉ, H., 1993, *New Methods of Celestial Mechanics*, Vol. 1, edited and introduced by Daniel L. Goroff, American Institute of Physics.

[29] HOLLE, A., WIEBUSCH, G., MAIN, J., HAGER, B., ROTTKE, H., and WELGE, K. H., 1986, *Phys. Rev. Lett.*, **56**, 2594.

[30] WINTGEN, D., and FRIEDRICH, H., 1987, *Phys. Rev.* A, **36**, 131.

[31] FRIEDRICH, H., and WINTGEN, D., 1989, *Phys. Rep.*, **183**, 37.

[32] WILSON, E. B., DECIUS, J. C., and CROSS, P. C., 1980, *Molecular Vibrations* (New York: Dover).

[33] GOMEZ LLORENTE, J. M., and POLLAK, E., 1992, *Ann. Rev. Phys. Chem.*, **43**, 91.

[34] DAVIS, M. J., 1993, *J. chem. Phys.*, **98**, 2614; DAVIS, M. J., 1995, *Int. Rev. Phys. Chem.*, **14**, 15.

[35] HELLER, E. J., 1981, *Accts. Chem. Res.*, **14**, 368.

[36] CHEN, Y., HALLE, S., JONAS, D. M., KINSEY, J. L., and FIELD, R. E., 1990, *J. opt. Soc. Am.* B, **7**, 1805.

[37] YAMANOUCHI, K., IKEDA, N., TSUCHIYA, S., JONAS, D. M., LUNDBERG, J. K., ADAMSON, G. W., and FIELD, R. W., 1991, *J. chem. Phys.*, **95**, 6330.

[38] JONAS, D. M., SOLINA, S. A. B., RAJARAM, B., SILBEY, R. J., FIELD, R. W., YAMANOUCHI, K., and TSUCHIYA, S., 1993, *J. chem. Phys.*, **99**, 7350.

[39] KÖPPEL, H., DOMCKE, W., and CEDERBAUM, L. S., 1984, *Adv. chem. Phys.*, Vol. 57 (New York: Wiley).

[40] MIYAWAKI, J., YAMANOUCHI, K., and TSUCHIYA, S., 1994, *J. chem. Phys.*, **101**, 4505.

[41] YAMANOUCHI, K., YAMADA, H., and TSUCHIYA, S., 1988, *J. chem. Phys.*, **88**, 4664.

[42] YAMANOUCHI, K., TAKEUCHI, S., and TSUCHIYA, S., 1989, *Prog. Theor. Phys.*, **98**, 420.

[43] YAMANOUCHI, K., TAKEUCHI, S., and TSUCHIYA, S., 1990, *J. chem. Phys.*, **92**, 4044.

[44] BROYER, M., DELACRETAZ, G., NI, G. Q., WHETTEN, R. L., WOLF, J.-P., and WÖSTE, L., 1989, *J. chem. Phys.*, **90**, 4620.

[45] GOMEZ LLORENTE, J. M., and TAYLOR, H. S., 1989, *J. chem. Phys.*, **91**, 953.

[46] YANG, X., RAGASHI, C. A., and WODTKE, A. M., 1990, *J. opt. Soc. Am.* B, **7**, 1835.

[47] YANG, X., ROGASKI, C. A., and WODTKE, A. M., 1990, *J. chem. Phys.*, **92**, 2111.

[48] FREEMAN, D. E., YOSHINO, K., ESMOND, J. R., and PARKINSON, W. H., 1984, *Planet. Space Sci.*, **32**, 239.

[49] JOHNSON, B. R., and KINSEY, J. L., 1987, *J. chem. Phys.*, **87**, 1525.

[50] JOHNSON, B. R., and KINSEY, J. L., 1989, *J. chem. Phys.*, **91**, 7638.

[51] CARRINGTON, A., and KENNEDY, R. A., 1984, *J. chem. Phys.*, **81**, 91.

[52] CARRINGTON, A., MCNAB, I. R., and WEST, Y. D., 1993, *J. chem. Phys.*, **98**, 1073.

[53] PIQUE, J. P., JOYEUX, M., MANNERS, J., and SITJA, G., 1991, *J. chem. Phys.*, **95**, 8744.

[54] THOMAN, J. W. JR, STEINFELD, J. I., MCKAY, R. I., and KNIGHT, A. E. W., 1987, *J. chem. Phys.*, **86**, 5909.

[55] DAI, H. L., KORPA, C. L., KINSEY, J. L., and FIELD, R. W., 1985, *J. chem. Phys.*, **82**, 1988.

[56] DAI, H. L., FIELD, R. W., and KINSEY, J. L., 1985, *J. chem. Phys.*, **82**, 2161.

[57] HARTMAN, P., 1964, *Ordinary Differential Equations* (New York: Wiley).

[58] FARKAS, M., 1994, *Periodic Motions*, Applied Mathematical Sciences, Vol. 104 (Berlin: Springer-Verlag).

[59] ARNOLD, V. I., 1978, *Mathematical Methods of Classical Mechanics*, Graduate Texts in Mathematics, Vol. 60 (Berlin: Springer-Verlag).

[60] MILNOR, J., 1963, *Morse Theory*, Annals of Mathematical Studies, Vol. 51 (Princeton University Press).

[61] BIRKHOFF, G. D., 1925, *Acta Math.*, **47**, 297.

[62] WEINSTEIN, A., 1973, *Inv. Math.*, **20**, 47.

[63] MOSER, J., 1976, *Commun. Pure Appl. Math.*, **29**, 727.

[64] YOSHIZAWA, T., 1975, *Stability Theory and the Existence of Periodic Solutions*, Applied Mathematical Sciences, Vol. 14 (Berlin: Springer-Verlag).

[65] RABINOWITZ, P. H., 1984, *SIAM J. math. Anal.*, **13**, 343.

[66] MACKAY, R. S., MEISS, J. D., and PERCIVAL, I. C., 1984, *Physica* D, **13**, 55.

[67] MACKAY, R. S., MEISS, J. D., and PERCIVAL, I. C., 1987, *Physica* D, **27**, 1.

[68] BENSIMON, D., and KADANOFF, L. P., 1984, *Physica* D, **13**, 82.

[69] FOUNARGIOTAKIS, M., FARANTOS, S. C., CONTOPOULOS, G., and POLYMILIS, C., 1989, *J. chem. Phys.*, **91**, 1389.

[70] HELLER, E. J., and DAVIS, M. J., 1980, *J. phys. Chem.*, **84**, 1999.

[71] DAVIS, M. J., 1988, *J. phys. Chem.*, **92**, 3124.

[72] WATERLAND, R. L., YUAN, J.-M., MARTENS, C. C., GILLILAN, R. E., and REINHARDT, W. P., 1988, *Phys. Rev. Lett.*, **61**, 2733.

[73] FARANTOS, S. C., FOUNARGIOTAKIS, M., and POLYMILIS, C., 1989, *Chem. Phys.*, **135**, 347.

[74] PROSMITI, R., FARANTOS, S. C., and TAYLOR, H. S., 1994, *Molec. Phys.*, **82**, 1213.

[75] LEFORESTIER, C., BISSELING, R., CERJAN, C., FEIT, M. D., FRIESNER, R., GULDBERG, A., HAMMERICH, A., JOLICARD, G., KARRLEIN, W., MEYER, H. D., LIPKIN, N., RONCERO, O., and KOSLOFF, R., 1991, *J. comput. Phys.*, **94**, 59.

[76] FEIT, M. D., and FLECK, J. A. JR, 1983, *J. chem. Phys.*, **78**, 301.

[77] FARANTOS, S. C., 1993, *Laser Chem.*, **13**, 87.

[78] SADEGHI, R., and SKODJE, R. T., 1995, *J. chem. Phys.*, **102**, 193.

[79] GOMEZ LLORENTE, J. M., ZAKRZEWSKI, J., TAYLOR, H. S., and KULANDER, K. C., 1989, *J. chem. Phys.*, **90**, 1505.

[80] TAYLOR, H. S., and ZAKRZEWSKI, J., 1988, *Phys. Rev. A*, **38**, 3732.

[81] HAZI, A. U., and TAYLOR, H. S., 1970, *Phys. Rev. A*, **1**, 1109.

[82] KOSLOFF, R., 1994, *Ann. Rev. Phys. Chem.*, **45**, 145.

[83] BARANGER, M., 1958, *Phys. Rev. A*, **111**, 481.

[84] WEISSMAN, Y., and JORTNER, J., 1982, *J. chem. Phys.*, **77**, 1486.

[85] MCDONALD, S. W., 1988, *Phys. Rep.*, **158**, 337.

[86] GOMEZ LLORENTE, J. M., and POLLAK, E., 1989, *J. chem. Phys.*, **90**, 5406.

[87] PRESS, W. H., FLANNERY, B. P., TEUKOLSKY, S. A., and VETTERLING, W. T., 1986, *Numerical Recipes* (Cambridge University Press).

[88] FEUDEL, U., and JANSEN, W., 1992, *Int. J. Bifurc. Chaos*, **2**, 773.

[89] MARCINEK, R., and POLLAK, E., 1994, *J. chem. Phys.*, **100**, 5894.

[90] AGUIAR, M. A. M., MALTA, C. P., BARANGER, M., and DAVIES, K. T. R., 1987, *Ann. Phys.*, **180**, 167.

[91] BARANGER, M., DAVIES, K. T. R., and MAHONEY, J. H., 1988, *Ann. Phys.*, **186**, 95.

[92] DAVIES, K. T. R., HUSTON, T. E., and BARANGER, M., 1992, *Chaos*, **2**, 215.

[93] DEUFLHARD, P., 1979, *Numer. Math*, **33**, 115.

[94] DEUFLHARD, P., 1974, *Numer. Math.*, **22**, 189.

[95] KELLER, H. B., 1976, *Numerical Solution of Two Point Boundary Value Problems*, Society for Industrial and Applied Mathematics, Vol. 24.

[96] STOER, J., and BULIRSCH, R., 1980, *Introduction to Numerical Analysis* (New York: Springer).

[97] SEYDEL, R., 1988, *From Equilibrium to Chaos: Practical bifurcation and stability analysis* (Amsterdam: Elsevier).

[98] REITHMEIER, E., 1991, *Periodic Solutions of Nonlinear Dynamical Systems*, Lecture Notes in Mathematics (Berlin: Springer-Verlag).

[99] NOCEDAL, J., 1992, *Acta Numerica* (Cambridge University Press).

[100] HENÓN, M., 1982, *Physica D*, **5**, 412.

[101] FARANTOS, S. C., 1992, *Time Dependent Quantum Molecular Dynamics*, edited by J. Broeckhove and L. Lathouwers (New York: Plenum), p. 27.

[102] BROUCKE, R. A., 1969, *NASA, Technical Report* No. 32-1360.

[103] CONTOPOULOS, G., FARANTOS, S. C., PAPADAKI, H., and POLYMILIS, C., 1994, *Phys. Rev. E*, **50**, 4399.

[104] PROSMITI, R., and FARANTOS, S. C., 1995, *J. chem. Phys.*, in press.

[105] YAKUBOVICH, V. A., and STARZHINSKII, V. M., 1975, *Linear Differential Equations with Periodic Coefficients*, Vol. 1 (Halsted Press).

[106] KRASNOSEL'SKII, M. A., and ZABREIKO, P. P., 1984, *Geometrical Methods of Nonlinear Analysis*, A series of comprehensive mathematics, Vol. 263 (Berlin: Springer-Verlag).

[107] NEWHOUSE, S. E., 1977, *Am. J. Math.*, **90**, 1061.

[108] NEWHOUSE, S. E., 1983, *Chaotic Behavior of Deterministic Systems*, edited by G. Iooss, R. H. G. Helleman and R. Stora (Amsterdam: North-Holland), p. 443.

[109] CONTOPOULOS, G., and POLYMILIS, C., 1993, *Phys. Rev. E*, **47**, 1546.

[110] ZEMBEKOV, A. A., 1994, *J. chem. Phys.*, **101**, 8842.

[111] SEYDEL, R., 1991, *Int. J. Bifurc. Chaos*, **1**, 3.

[112] ALLGOWER, E. L., and GEORG, K., 1993, *Numerical Continuation Methods, Springer series in computational mathematics, Vol. 13* (Berlin: Springer-Verlag).

[113] ALLGOWER, E. L., and GEORG, K., 1993, *Acta Numerica* (Cambridge University Press).

[114] MURRELL, J. N., CARTER, S., FARANTOS, S. C., HUXLEY, P., and VARANDAS, A. J. C., 1984, *Molecular Potential Energy Functions* (New York: Wiley).

[115] VEGIRI, A., and FARANTOS, S. C., 1993, *J. chem. Phys.*, **98**, 4059.

[116] FARANTOS, S. C., KAPETANAKIS, S., and VEGIRI, A., 1993, *J. phys. Chem.*, **97**, 12158.

[117] FARANTOS, S. C., 1994, *Z. Phys.* D, **31**, 213.

[118] EGGEN, B. R., MARKS, A. J., MURRELL, J. N., and FARANTOS, S. C., 1994, *Chem. Phys. Lett.*, **219**, 247.

[119] FARANTOS, S. C., 1992, *Chaotic Dynamics: Theory and Practice*, edited by T. Bountis (New York: Plenum), p. 301.

[120] CONTOPOULOS, G., 1970, *Astron. J.*, **75**, 96.

[121] FOUNARGIOTAKIS, M., FARANTOS, S. C., and TENNYSON, J., 1988, *J. chem. Phys.*, **88**, 1598.

[122] FARANTOS, S. C., and FOUNARGIOTAKIS, M., 1990, *Chem. Phys.*, **142**, 345.

[123] FARANTOS, S. C., GOMEZ LLORENTE, J. M., HAHN, O., and TAYLOR, H. S., 1990, *J. chem. Phys.*, **93**, 76.

[124] BENTLEY, J. A., BRUNET, J.-P., WYATT, R. E., FRIESNER, R. A., and LEFORESTIER, C., 1989, *Chem. Phys. Lett.*, **161**, 393.

[125] BARONAVSKI, A. P., 1979, *Chem. Phys. Lett.*, **61**, 532.

[126] FARANTOS, S. C., and ZACHILAS, L., 1993, *Molec. Phys.*, **80**, 1499.

[127] CARTER, S., HANDY, N. C., and MILLS, I. M., 1990, *Phil. Trans. R. Soc. Lond.* A, **332**, 309.

[128] FARANTOS, S. C., and TAYLOR, H. S., 1991, *J. chem. Phys.*, **94**, 4887.

[129] LE QUÉRÉ, F., and LEFORESTIER, C., 1991, *J. chem. Phys.*, **94**, 1118.

[130] BALAKRISHNAN, N., and BILLING, G. D., 1994, *J. chem. Phys.*, **101**, 2968.

[131] FARANTOS, S. C., 1992, *Chem. Phys.*, **159**, 329.

[132] FARANTOS, S. C., 1995, *J. molec. Struct. THEOCHEM* (to be published).

[133] SCHINKE, R., and ENGEL, V., 1990, *J. chem. Phys.*, **93**, 3252.

[134] KULANDER, K. C., CERJAN, C., and OREL, A. E., 1991, *J. chem. Phys.*, **94**, 2571.

[135] EZRA, G., RICHTER, K., TANNER, G., and WINTGEN, D., 1991, *J. Phys. B*, **24**, L413.

[136] MÜLLER, J., BURGDÖRFER, J., and NOID, D., 1992, *Phys. Rev. A*, **45**, 1471.

[137] FARANTOS, S. C., and MURRELL, J. N., 1981, *Chem. Phys.*, **55**, 205.

[138] FREDERICK, J. H., McCLELLAND, G. M., and BRUMER, P., 1985, *J. chem. Phys.*, **83**, 190.

[139] See the articles in issue. 1990, *J. opt. Soc. Am.* B, **7**, 1802–1970.

[140] ZACHILAS, L., and FARANTOS, S. C., 1991, *Chem. Phys.*, **154**, 55.

[141] FARANTOS, S. C., and TENNYSON, J., 1988, *Fractals, Quasicrystals, Chaos, Knots, and Algebraic Quantum Mechanics*, edited by L. S. Cederbaum, A. Amann, and W. Gans (Dordrecht: Kluwer), p. 195.

[142] POLLAK, E., 1985, *Theory of Chemical Reaction Dynamics*, Vol. 3, edited by M. Baer (Boca Raton, FL: CRC), p. 123.

[143] HAHN, O., and TAYLOR, H. S., 1992, *J. chem. Phys.*, **96**, 5915.

[144] HAHN, O., GOMEZ LLORENTE, J. M., and TAYLOR, H. S., 1991, *J. chem. Phys.*, **94**, 2608.

[145] GOMEZ LLORENTE, J. M., and POLLAK, E., 1987, *Chem. Phys. Lett.*, **138**, 125.

[146] TENNYSON, J., 1995, *Rep. Prog. Phys.*, **57**, 421.

[147] GARCIA, G., and TENNYSON, J., 1994, *Molec. Phys.*, **83**, 361.

[148] HINDE, R. J., BERRY, R. S., and WALES, D. J., 1992, *J. chem. Phys.*, **96**, 1376.

[149] NEZIS, A., and FARANTOS, S. C. (unpublished results).

[150] SEPULVEDA, M. A., BADDI, R., and POLLAK, E., 1989, *Phys. Rev. Lett.*, **63**, 1226.